Journal of Magnetism and Magnetic Materials 547 (2022) 168833

Contents lists available at ScienceDirect

Journal of Magnetism and Magnetic Materials

journal homepage: www.elsevier.com/locate/jmmm

Research articles

Ferromagnetic $CeSi_{1.2}Ga_{0.8}$ alloy: Study on magnetocaloric and thermoelectric properties

K. Synoradzki [a], P. Skokowski [a], Ł. Frąckowiak [a], M. Koterlyn [b], J. Sebesta [c], D. Legut [c], T. Toliński [a,*]

[a] Institute of Molecular Physics, Polish Academy of Sciences, Poznań, Poland
[b] Institute of Physics, K. Wielkiego University, Bydgoszcz, Poland
[c] IT4Innovations, VSB – Technical University of Ostrava, Czech Republic

ARTICLE INFO

Keywords:
$CeSi_{1.2}Ga_{0.8}$
Kondo system
Seebeck effect
Competing energy scales
Magnetocaloric effect

ABSTRACT

We present the magnetic, specific heat, electrical resistivity, and thermoelectric power measurements for the intermetallic compound $CeSi_{1.2}Ga_{0.8}$. This composition belongs to the series $CeSi_{2-x}Ga_x$, which exhibits diverse magnetic orderings and different crystallographic structures depending on the substitution level x. It has been previously suggested that for $0.0 < x < 1.3$ the compounds crystallize in the α-$ThSi_2$ type structure and for $0.7 < x < 1.3$ they order ferromagnetically below 14 K. Our complementary studies for $x = 0.8$ reveal that it is a complex system due to the Kondo scattering competing with the RKKY interactions. The transition from the paramagnetic to the ferromagnetic state takes place at $T_C = 12.5(1)$ K. Moreover, the Seebeck coefficient and electrical resistivity show not only an anomaly related to the magnetic transition, but also a broad maximum at ~90 K related to the crystal field effect. The case of $x = 0.8$ is of special interest as it is at the crossing of the characteristic temperatures, i.e. T_{ord} (magnetic ordering temperature) ~ T_K (Kondo temperature) ~10 K. Additionally, *ab initio* electronic structure calculations were performed allowing us to determine phase stability, (revealing two stable phases - α-$GdSi_2$-type and α-$ThSi_2$-type structures) as well as spin and orbital moment decomposition on Ce-states for both considered structures.

1. Introduction

The binary compound $CeSi_2$ is a known Kondo system with a non-magnetic ground state and moderate electronic specific heat coefficient, $\gamma \sim 100$ mJ/K [1–4], hence it cannot be unambiguously classified as heavy fermion system. On the other hand, $CeGa_2$ exhibits a cascade of magnetic phase transitions at 11.3, 10.3, 9.9, and 8.4 K [5–8]. These compounds crystallize in various structures. While the $CeSi_2$ compound crystallizes in the tetragonal α-$ThSi_2$ type structure (space group $I4_1/amd$, No. 141), the Ga-based compound crystallizes in the hexagonal AlB_2-type structure (space group $P6/mmm$, No. 191) [6,8–10].

The series $CeSi_{2-x}Ga_x$ exhibits various magnetic ordering and different crystallographic structures depending on the substitution level x [5,11–17]. It has been previously suggested that for $0.0 < x < 1.3$ the compounds crystallize in the α-$ThSi_2$-type structure and for $0.7 < x < 1.3$ [11,17] they exhibit ferromagnetic (FM) ordering [12,14]. Due to the influence of the crystal field (CF) this range of Ga content is known to require the characterization of the physical properties by two Kondo temperatures, the high one, T_K^h, and the low one, T_K^l, interrelated by $T_K^h = (T_K^l \Delta_1 \Delta_2)^{1/3}$, where Δ_1 and Δ_2 are the energies of the CF excitations. For $x = 0.7$ $T_K^l = 9.6$ K and for $x = 1.0$ $T_K^l = 18$ K [15,18]. These magnitudes of the Kondo energy scale are comparable to the magnetic energy scale, corresponding to the RKKY interaction and manifested as an appearance of the magnetic ordering at T_{ord} ~10 K. Therefore, $CeSi_{1.2}Ga_{0.8}$ is one of the most interesting, yet not widely studied, representatives of the $CeSi_{2-x}Ga_x$ series. The competition between the Kondo and RKKY interactions might cause the untypical behavior of various measured quantities at or around the temperature of magnetic ordering. Magnetocaloric effect (MCE) and thermoelectric properties have been intensively studied in recent years due to the ideas of substitution of the classical gas-based fridges and air-conditioners with environment friendly alternatives [19,20]. Moreover, the energy harvesting has become a promising perspective to recover the heat dissipated all around. Apart from the experimental search for novel materials, theoretical studies of physical properties of numerous materials are widely carried out, including Monte Carlo methods [21,22] or

* Corresponding author.
E-mail address: tomtol@ifmpan.poznan.pl (T. Toliński).

https://doi.org/10.1016/j.jmmm.2021.168833
Received 23 July 2021; Received in revised form 18 October 2021; Accepted 13 November 2021
Available online 18 November 2021

simulations using the First Order Reversal Curve tool (FORC) [23]. Our investigations concern experimental characterizations of intermetallic compounds and alloys based on anomalous lanthanides, especially Ce-based ones.

In this article, we present an extended research for the case of x = 0.8, which has not been studied previously and we find it is of a special interest. The competition between Kondo effect, RKKY interactions, and CF excitations might provide interesting physical properties at low temperatures [4]. Therefore, in the present study we verify magnetic and transport properties of $CeSi_{1.2}Ga_{0.8}$. The study includes the magnetocaloric parameters analysis, as well as thermoelectric power, electrical resistivity, thermal conductivity, magnetic and specific heat measurements, supported by *ab initio* calculations of the energy of formation for both crystal structures. Moreover, these first principle calculations provide insight into the density of states and the magnetic moments.

2. Experimental

A polycrystalline sample of a nominal composition $CeSi_{1.2}Ga_{0.8}$ was prepared by arc melting the constituent elements of high purity in an argon atmosphere. The sample was melted several times and rotated after each melting process. Weight losses after melting were below 0.5 mass%. After synthesis the compound was annealed at 900 °C for 120 h.

The sample quality was examined via the powder x-ray diffraction (XRD) using the PANalytical X'Pert Pro with a Cu Kα monochromator. Rietveld refinements were performed using the program FullProf [24]. The density of the obtained sample was determined using the Archimedes method.

Scanning electron microscopy (SEM) images and the elemental composition was obtained using FEI Nova NanoSEM 650 with the energy dispersive spectroscopy (EDS) Bruker detector. Electron energy of 30 keV was used for imaging and to excite the characteristic radiation of the elements. Analysis of the EDS data was performed with a license software delivered with the instrument using P/B ZAF (standardless) method.

All other physical property measurements were made in the temperature range from 2 to 400 K and in magnetic fields up to 9 T on the PPMS platform (Quantum Design) equipped with appropriate options. We measured the magnetic properties with a vibrating sample magnetometer (VSM) and an AC Measurement System (ACMS). Transport measurements were carried out on a cuboidal sample with dimensions of 1 mm × 1 mm × 8 mm, which was cut with a wire saw (WS-21 K.D. UNIPRESS). The contacts were made with a silver paste.

Complementary to the experimental measurements, the *ab initio* electronic structure calculations were performed. Due to an off-stoichiometric composition of the studied compounds, a fully relativistic Korringa-Kohn-Rostoker (KKR) method implemented in the SPR-KKR package was employed [25,26]. It is based on the multiple scattering theory and Green's function formalism, which allows to treat the chemical disorder with a high efficiency by means of the coherent potential approximation. The calculations were performed in the *spdf*-atomic model and the xc-potential of Vosko, Wilk, Nusair was involved [27]. To treat the electron correlations for Ce *f*-states LDA + *U* approach in the atomic-like limit [28] was employed. The calculations were treated in the irreducible part of the 12ˆ3 *k*-point large Brillouin zone using the integration of over 30 energy points in the complex energy plane.

3. Results and discussion

Previous reports performed on polycrystalline samples, have shown that for 0.0 < x < 1.3 the compounds $CeSi_{2-x}Ga_x$ crystallize in the tetragonal α-$ThSi_2$ type structure (space group $I4_1/amd$, No. 141). Recent studies by Darone *et al.* on single crystal have also confirmed that the compound $CeSi_{1.13}Ga_{0.87}$ crystallizes in the α-$ThSi_2$ type structure [16]. Using this information we fitted our data, obtaining a good match [Fig. 1(a)]. We identified a small amount (~8%) of gallium oxide β-Ga_2O_3, as an impurity [29]. A mismatch occurs in the intensity of individual peaks, which may be related to the texture of the sample or to a structural disorder [30]. The obtained values of the lattice parameters (a = 4.2381(2) Å, c = 14.170(1) Å) are in good agreement with those known from the literature for similar alloys of this series [12,15,17]. Nevertheless, we decided to make additional fits using other models of crystallographic structures. From our *ab initio* calculations (see below) it turns out that the orthorhombic α-$GdSi_2$-type structure (space group *Imma*, No. 74) possesses lower formation energy than the tetragonal α-$ThSi_2$-type. The orthorhombic α-$GdSi_2$-type structure was previously observed in a similar system containing Ge, $CeSi_{2-x}Ge_x$ [17], in Y doped compound $Y_{0.5}Ce_{0.5}Si_2$ [4], or in samples containing heavy rare earth elements $RESi_{2-x-y}Ga_x$ (*RE* = Ho, Er, Tm) [16]. The structural parameters determined from our fits for $CeSi_{1.2}Ga_{0.8}$ are summarized in Table 1. Since both structures are very similar to each other (the α-$GdSi_2$–type structure can be regarded as a slightly deformed structure of α-$ThSi_2$-type), both fits give very similar results. However, the values of the Bragg factor and structure factor (R_B and R_F) for the α-$ThSi_2$-type structure are slightly smaller than for the α-$GdSi_2$-type structure, which might suggest that this structure is the correct one. On the other hand, the difference is small. Unfortunately, the quality of our data does not allow us to clearly determine which structure is appropriate for our sample. To precisely settle this, detailed studies on high-quality single crystalline samples are needed, carried out with the use of more precise measuring instruments.

The density of our sample was determined by the Archimedes method and is equal to 5.92(1) g/cm^3. This value is smaller than that determined from the crystallographic data for orthorhombic α-$GdSi_2$-type structure (5.985 g/cm^3), which may result from imperfections like voids and cracks in the polycrystalline samples. On the other hand, the experimental value almost perfectly matches the theoretical value for the tetragonal α-$ThSi_2$-type structure (5.908 g/cm^3), indicating that it is

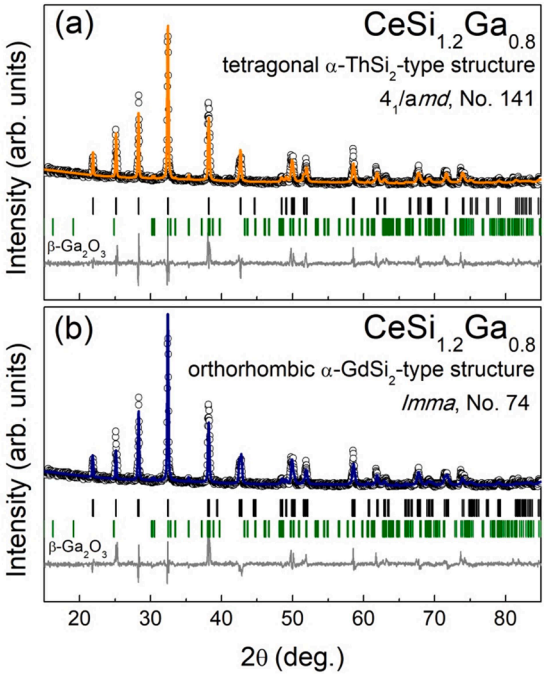

Fig. 1. Room temperature X-ray diffraction pattern of $CeSi_{1.2}Ga_{0.8}$ alloy. Open circles show observed data and solid line represents the Rietveld refined patterns (a) for tetragonal α-$ThSi_2$-type and (b) for orthorhombic α-$GdSi_2$-type structure. The difference patterns are shown as gray solid bottom lines. The Bragg peaks for α-$ThSi_2$-type, α-$GdSi_2$-type structure, and β-Ga_2O_3 impurity phase are marked by short vertical lines.

Table 1
Structural parameters of $CeSi_{1.2}Ga_{0.8}$ sample.

Sample	$CeSi_{1.2}Ga_{0.8}$	
Space group	$I4_1/amd$, No. 141	*Imma*, No. 74
Cell parameters	$a = 4.2381(2)$ Å	$a = 4.2506(3)$ Å
	$b = a$	$b = 4.2260(3)$ Å
	$c = 14.170(1)$ Å	$c = 14.174(1)$ Å
Cell volume	$V = 254.52(2)$ Å^3	$V = 254.62(3)$ Å^3
Atom positions		
Ce (x, y, z)	0.0, 0.75, 0.125	0.0, 0.25, 0.623(1)
Si/Ga1 (x, y, z)	0.0, 0.25, 0.464(1)	0.0, 0.25, 0.050(1)
Si/Ga2 (x, y, z)	–	0.0, 0.25, 0.212(7)
Theoretical density	5.908	5.985
R_B	12.8	19.3
R_F	11.0	12.4
β -Ga_2O_3 phase content	8(1)%	5(1)%

the accurate structure.

To verify the stoichiometry and presence of secondary phases we carried out the SEM and EDS measurements. Fig. 2 shows the obtained results. The SEM images [Fig. 2(a)] showed that the sample was free from major imperfections, although we did observe a few gaps and micro-cracks. The EDS were performed on large areas in several places of the sample. The experimental results revealed the stoichiometry of $Ce_{0.97(5)}Si_{1.17(2)}Ga_{0.86(2)}$, which is in good agreement with the nominal concentration. The mapping showed that apart from the regions where all three elements are uniformly distributed, there are grain boundary precipitates that are rich in Si and Ga [Fig. 2(c) and (d)]. SEM and EDS measurements showed that our sample consists of quite large and irregularly shaped grains, in which size varies in the range from several dozen to several hundred micrometers.

The temperature dependence of the magnetization (Fig. 3) allowed us to confirm the occurrence of the magnetic phase transition at T_C = 12.5(1) K, which was determined from the derivative of the magnetization as a function of temperature, dM/dT, see inset (b) in Fig. 3. The determined value of T_C is close to that reported in the literature for $CeSi_{2-x}Ga_x$ group of alloys, where T_C is 12 K and 7 K for x equal to 0.7 and 1.0, respectively [15], and T_C ~12.5 K from extrapolation to x = 0.8 of the plot presented by Moshchalkov *et al.* [12]. These slight differences in the magnetic ordering temperature for samples from different authors with theoretically the same chemical composition are probably due to different actual stoichiometry of different samples. However, the chemical composition was not verified with EDS in previous works [12,15]. Additionally, the zero field cooling (ZFC) curve clearly shows a slope change at 5 K. This may be related to a presence of a small antiparallel component of the magnetic moment or come from an additional

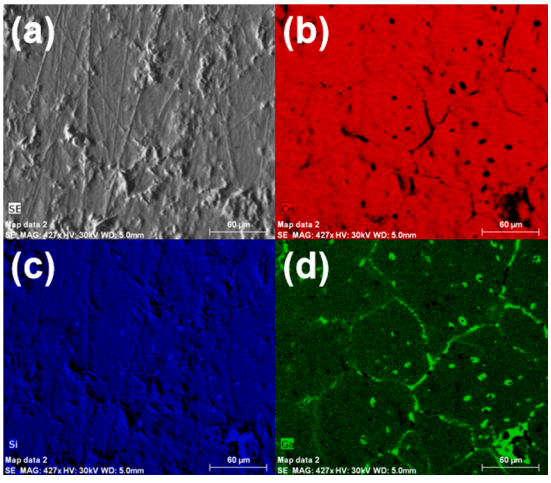

Fig. 2. SEM image (a) and elemental EDS maps (b, c, d) recorded for $CeSi_{1.2}Ga_{0.8}$ alloy.

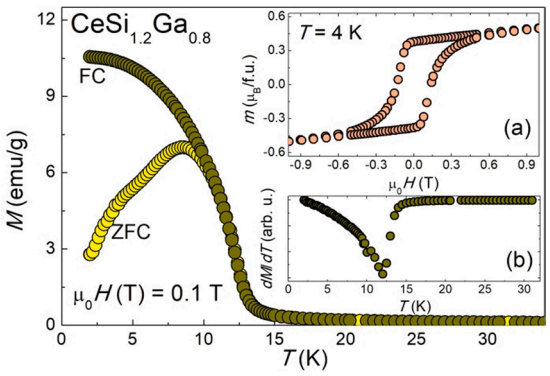

Fig. 3. Magnetic properties of $CeSi_{1.2}Ga_{0.8}$ alloy. Zero field cooled (ZFC) and field cooled (FC) magnetization versus temperature curves measured with an applied magnetic field of $\mu_0 H$ = 0.1 T. Inset (a) shows the hysteresis loop measured at 4 K and inset (b) indicates T_C = 12.5(1) K determined on the dM/dT(T) curve.

phase. To explain this, we preformed measurements of the AC magnetic susceptibility. In the real χ' and imaginary χ" parts of magnetic susceptibility (Fig. 4) we observed two sharp peaks of different intensity. The appearance of distinct peaks in χ" excludes the occurrence of the antiferromagnetic ordering in this sample [31]. The first peak, the stronger one, is located around ~ 3 K, and is related to the FM ordering of our sample. The second peak, the smaller one, is located around 8 K, and it's position coincides with the ZFC curve maximum in DC magnetization (Fig. 3). The origin of this peak is unclear. It may come from an impurity phase, e.g. $CeGa_2$ phase or from CeSiGa phase, which has a FM transition at ~8 K [15,18]. On the other hand, in the XRD and SEM/EDS measurements we do not see any traces of this phases. Therefore, this peak may be related to the change in the arrangement of the magnetic moments, which is often observed in similar compounds and alloys [32]. Notwithstanding to confirm this, additional measurements are needed,

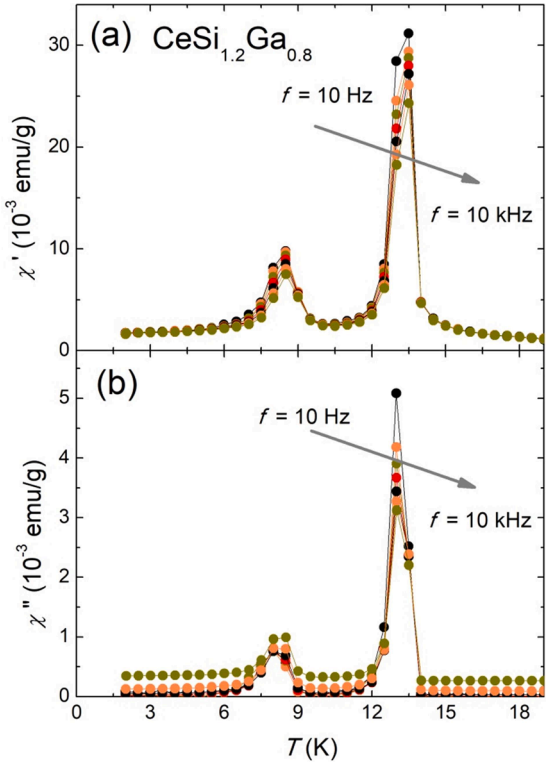

Fig. 4. Real part χ' (a) and imaginary part χ" (b) of AC magnetic susceptibility measured at various frequencies (10–10 000 Hz range) for $CeSi_{1.2}Ga_{0.8}$ alloy.

e.g. neutron diffraction. Slight changes in the observed χ' and χ" peaks (shape, intensity or position) as a function of the frequency of the external magnetic field (Fig. 4) can be related to the movement of the domain walls [31].

The magnetization curve $M(\mu_0 H)$ indicates that the $CeSi_{1.2}Ga_{0.8}$ alloy is a hard FM with a coercive field of the order of 0.14(1) T at 4 K. At 4 K and 9 T the magnetization reaches 0.96 μ_B/f.u. and is a value lower than that expected for the Ce^{3+} ion ($g_J J = 2.14\ \mu_B$). This lower value of the saturation moment may suggest antiferromagnetic interactions or a strong influence of anisotropy [33]. Also, the influence of the crystal field can lead to a decrease in the value of the saturation moment [34].

As the $CeSi_{1.2}Ga_{0.8}$ alloy exhibits a ferromagnetic ordering, we decided to determine its magnetocaloric response in order to assess its application potential. For this purpose we measured the magnetization curves in isothermal conditions around the transition temperature. We present the results of these measurements in the form of an Arrott plot in Fig. 5(a) [35]. Then, basing on the Maxwell relations, we used the equation [36]

$$\Delta S_M(T, \mu_0 H) = \int_0^{\mu_0 H^{MAX}} \frac{\partial M(T, \mu_0 H)}{\partial T} d\mu_0 H \quad (1)$$

to estimate the magnetic entropy change ΔS_M as a function of temperature for several different values of the magnetic field changes $\mu_0 \Delta H$ [Fig. 5(b)]. The maximum ΔS_M value −6.5(1) J/(kg K) is reached for the $\mu_0 \Delta H = 5$ T at T_C. This value is more than two times lower than for the antiferromagnetic compound CeSi (ΔS_M = -13.7 J/kg K for $\mu_0 \Delta H = 5$ T), which is a good representative of a magnetocaloric material in the low temperature range [37]. On the other hand, it is comparable to the values obtained for the RGa_2 series (e.g. for $DyGa_2$ ΔS_M = -6.5 J/(kg K) for $\mu_0 \Delta H = 5$ T) [38]. Another parameter describing the MCE is the relative cooling power (RCP = $|\Delta S_M{}^{MAX}| \cdot \delta T_{FWHM}$), where $|\Delta S_M{}^{MAX}|$ is the absolute maximum ΔS_M value and δT_{FWHM} is the half-width of the $\Delta S_M(T)$ peak [36]. Maximum values of RCP as a function of the change in the external magnetic field are plotted in Fig. 5(c) (right axis). Both the ΔS_M and the RCP values as a function of the magnetic field changes show exponential type relationships $\sim \mu_0 \Delta H^n$, but with different values of exponents. Fits allowed to estimate the values of these exponents (n), which are equal to 0.81(1) and 1.16(3), for ΔS_M and RCP, respectively. The obtained n values are close to those predicted by the mean-field theory (2/3 and 4/3) [39].

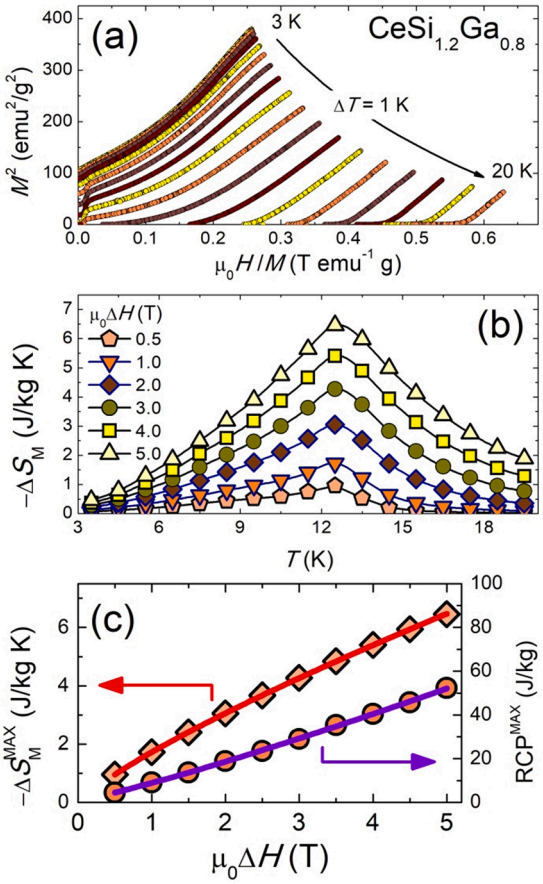

Fig. 5. (a) Arrott plot of M^2 vs. $\mu_0 H/M$ at temperatures in the vicinity of T_C. (b) Temperature dependence of the magnetic entropy change ΔS_M under different applied magnetic field values for $CeSi_{1.2}Ga_{0.8}$. (c) The maximal entropy change (left axis) and maximal RCP (right axis) vs. magnetic field change $\mu_0 \Delta H$. The solid lines represent fits with the power law $\sim \mu_0 \Delta H^n$.

The transition from paramagnetic to ferromagnetic state is also evident in the specific heat (C_p) data (Fig. 6), where a typical anomaly occurs at around 12 K. Moreover, below this transition there is another one located near 8 K, as it was also observed in magnetization measurements (Fig. 4). The extrapolation of the C_p/T vs. T data to the lowest temperatures allows to determine the Sommerfeld coefficient γ and Debye temperature Θ_D using the following expression: $C_p = \gamma T^2 + 12/5\pi^4 nR(T/\Theta_D)^3$. Unfortunately, due to the proximity of the magnetic phase transition, the γ value may be burdened with a significant error. Nevertheless, the value obtained by us is equal to γ = 20(2) mJ/(mol K^2) and is slightly lower than those reported in the literature for similar alloys (for $CeGa_{1.75}Si_{0.25}$ γ = 210 mJ/(mol K^2), for $CeGa_2$ γ = 340 mJ/(mol K^2)) [5]. The electronic density of states $N(E_F)$ at the Fermi level, calculated by the formula [40] $\gamma = k_B{}^2 \pi^4 N(E_F)/3$, is equal to 8.5 states/(eV atom). This value is in good agreement with those obtained in the *ab initio* calculations (see Fig. 8). The Debye temperature is equal to 78.9(2) K. Around room temperature C_p reaches value provided by the classical Dulong-Petit law (3nR) [40].

The temperature dependence of the electrical resistance ρ(T) shows the metallic nature for our sample. The obtained value of the residual resistivity ratio, $RRR = \rho(300\ K)/\rho(T)$, is about ~1.5, which is a typical value for multicomponent polycrystalline samples. Only one steep drop in resistivity [Fig. 7(a)] was registered at temperature ~13 K, consistent with the magnetic ordering confirmed by magnetization and specific heat measurements. The second anomaly around 8 K is not visible in the ρ(T). The low-temperature resistivity, below T_C, can be well described by the expression [41–43]:

$$\rho(T) = \rho_0 + A\Delta_R T\left[1 + 2\frac{T}{\Delta_R}\right] exp\left(\frac{-\Delta_R}{T}\right), \quad (2)$$

where the first term (ρ_0) represents scattering of conduction electrons on crystal lattice imperfections, while the second term accounts for scattering on FM spin-wave excitations with the energy gap Δ_R in the magnon spectrum. The coefficient A is a fitting parameter related to the

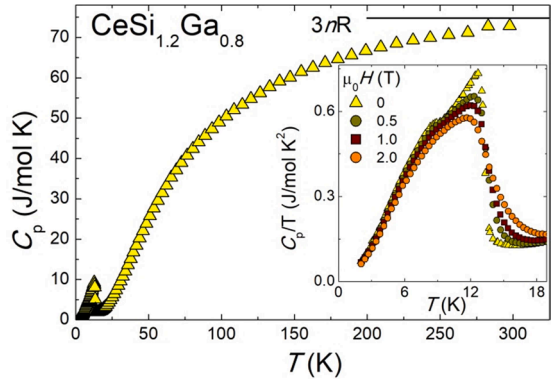

Fig. 6. Temperature dependence of the specific heat of $CeSi_{1.2}Ga_{0.8}$ alloy. The solid line represents the Dulong-Petit limit (3nR). The inset shows C_p/T vs. T in the low temperature range measured in zero and finite magnetic field.

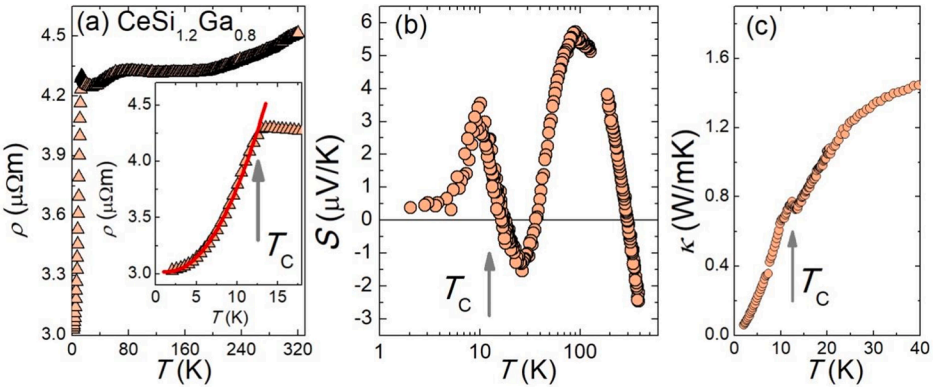

Fig. 7. Transport properties for the $CeSi_{1.2}Ga_{0.8}$ sample. (a) Electrical resistivity. Inset shows the temperature range close to the phase transition. The solid line represents the fitting with equation (2) (for details see text). (b) Seebeck coefficient. Note a logarithmic x-axis scale. (c) Thermal conductivity in the range of low temperatures. The arrow indicates the position of T_C.

spin-wave stiffness [41,44]. The parameters values obtained from the fitting are $\rho_0 = 3.02(1)$ μΩm, $A = 5.2(2) \times 10^{-3}$ μΩmK^{-2}, and $\Delta_R = 5.8(9)$ K. Apart from the anomaly near the magnetic phase transition, the $\rho(T)$ dependence reveals a broad maximum at ~80 K. It is developed by the CF effect expected for the localized *f* states of cerium. It has been also interpreted in terms of the high, T_K^h, and low, T_K^l, Kondo temperature [14,15]. The high Kondo temperature implies that the entire $J = 5/2$ multiplet is involved in the scattering process and $T_K^h = (T_K^l \Delta_1 \Delta_2)^{1/3}$. The small increase of the resistivity with lowering the temperature in the region just above the magnetic ordering temperature is probably caused by the proximity to T_K^l, i.e. by the Kondo effect.

Fig. 7(b) shows thermoelectric power *S* as a function of temperature and it distinctly illustrates the characteristic energy scales governing the properties of $CeSi_{1.2}Ga_{0.8}$. The Seebeck coefficient shows three extremes: two positive at ~10 K and ~90 K, and one negative at ~25 K. The peaks are in accordance with the high, T_K^h, and low, T_K^l, Kondo temperatures related by the CF energies: $T_K^h = (T_K^l \Delta_1 \Delta_2)^{1/3}$. The maximum value of the Seebeck coefficient is typical of metals (~6 μV/K at ~80 K). Also, the value of the thermoelectric power factor, $PF = S^2/\rho$, is also small, reaching a maximum value of 7.5(1) μW/(mK^2) at ~80 K. The *PF* value in the vicinity of the magnetic transition is even smaller 3.3 (1) μW/(mK^2) at 10 K. The thermal conductivity (κ) [Fig. 7(c)] for the $CeSi_{1.2}Ga_{0.8}$ alloy is relatively low, possibly due to the small size of the crystallites, the macroscopic imperfections in the form of voids and cracks, and the structural disorder caused by Ga for Si substitution. Above 150 K, the value of κ is dominated and overestimated by the influence of radiation losses, typical for this type of measurements [45]. At the lowest temperatures in the κ(*T*) dependence, we observe a single clear anomaly around 13 K, which is related to the magnetic phase transition.

Using the above data, we can determine the thermoelectric figure of merit $ZT = TS^2/\rho\kappa$, which at 80 K is 3.8×10^{-4}. This value is small but comparable to other Ce-based materials [4,46].

Finally, we decided to test if the tetragonal structure is the most stable one for this chemical composition. Thus, we employed *ab initio* SPR-KKR [25,26] calculation to determine a ground state energy difference between two considered crystal structures. Initially, we did not consider Hubbard model, i.e., *U* and *J* parameters [27]. It revealed that the orthorhombic α-$GdSi_2$-type structure (space group *Imma*, No. 74) possesses formation energy lower by about 81.6 meV/atom than the tetragonal α-$ThSi_2$-type (space group $I4_1/amd$, No. 141) one. It was confirmed also by calculations employing Perdew-Burke-Ernzerhof parametrized generalized gradient approximation (PBE) [28]. However, both yielded almost zero total magnetic moments which is inconsistent with the experimental observations (Table 2). Therefore, a Hubbard model was employed, i.e., non-zero *U* and *J* parameters were introduced in our calculations to act on the Ce *f*-states, which are located near the Fermi level and are responsible, to the largest extent, for the magnetic behavior of the studied compounds. It enabled us to achieve magnitudes of the total magnetic moment corresponding to the experimentally determined magnetization, as especially the orbital moment was enhanced. Regarding the *Imma* and $I4_1/amd$ space group structures and employing $U = 1.30$ eV and $J = 0.25$ eV, we obtained a total magnetic moment of 1.27 μ_B and 1.08 μ_B, respectively. Even for the calculations of the correct magnetic moments using the Hubbard *U* model, the former *Imma* space group still has a lower formation energy, keeping nearly the original value despite *U*, *J*-magnitude variation as well.

Table 2
Magnitudes of the magnetic moments of Ce atom for both crystal structures with and without the Hubbard model (*U* and *J* parameters).

U (eV)	*J* (eV)	*Imma* (No. 74)			$I4_1/amd$ (No. 141)		
		μ_S (μ_B)	μ_L (μ_B)	μ_{total} (μ_B)	μ_S (μ_B)	μ_L (μ_B)	μ_{total} (μ_B)
–	–	−0.55	0.42	−0.13	−0.59	0.45	−0.14
1.30	0.25	−0.78	2.05	1.27	−0.76	1.84	1.08

The densities of states plotted for both considered structures are quite similar (Fig. 8). They are dominated by Ce 4*f* states nearby the Fermi level. Likely, the only significant difference is a distinct behavior of Si states. In contrast to the $I4_1/amd$ space group, the *Imma* one possesses two different Si states, which do not behave exactly in the same way. Hybridization of the Si *p*, *d*-states with Ce *f*-states is likely responsible for a bump in the minority channel in the vicinity of the Fermi level.

4. Summary

In this work, we investigated the physical properties of the polycrystalline sample of the $CeSi_{1.2}Ga_{0.8}$ alloy, which belongs to the $CeSi_{2-x}Ga_x$ series, where the interplay between different effects leads to interesting physical properties. Our measurements showed that this alloy exhibits a ferromagnetic order with $T_C = 12.5(1)$ K. We also observed an additional magnetic phase transition at ~8 K. It may be an intrinsic feature of a given material or it may come from a contamination with a different phase, and to clarify this, additional measurements are essential. In the next step, we performed an analysis of the magnetocaloric parameters. Using isothermal magnetization measurements, we determined the magnetic entropy change $\Delta S_M(T)$, which is a measure of the magnetocaloric effect. The obtained values are not high, −6.5(1) J/(kg K) for $\mu_0 \Delta H = 5$ T, but comparable with other materials of this type in this temperature range.

The electrical transport and thermopower properties of this material

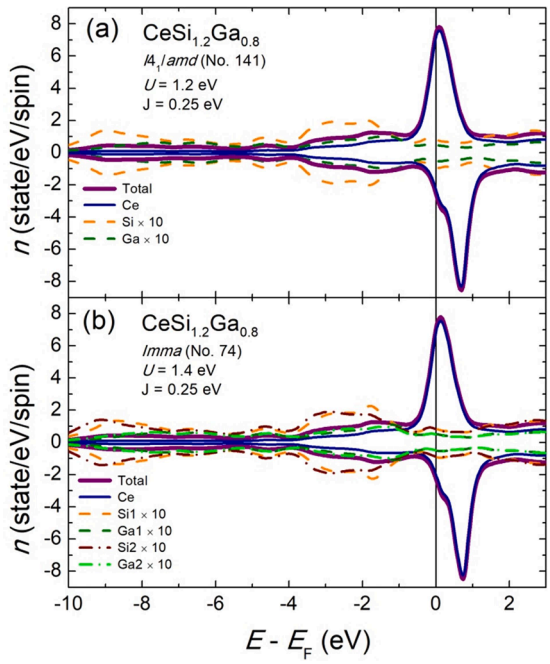

Fig. 8. The densities of states (DOS) of $CeSi_{1.2}Ga_{0.8}$ for (a) $I4_1/amd$ (141) and (b) *Imma* (74) crystal structure.

are governed by an interplay between Kondo, magnetic RKKY, and CF interactions. Additionally, transport measurements allowed us to determine the strength of the thermoelectric effect in this alloy. Values characterizing the thermoelectric effect ($PF = 7.5(1)$ μW/(mK^2)), $ZT = 3.8 \times 10^{-4}$ at ~80 K) also do not reach significant values, which is typical for this type of materials.

Experimentally, at this moment, we are not able to resolve which of the two similar structures is the ground-state one. However, from our theoretical calculations it is clear that the orthorhombic *Imma* (74) structure is energetically more favored, by 81.6 meV/atom, than the tetragonal $I4_1/amd$ (141) one, irrespective of the use of the Hubbard model. In addition, based on the determined electronic structure, we showed the decomposition of the total moment into the spin and orbital contribution.

CRediT authorship contribution statement

K. Synoradzki: Conceptualization, Methodology, Validation, Investigation, Data curation, Writing – original draft, Visualization. **P. Skokowski:** Investigation, Data curation, Visualization, Writing – review & editing. **Ł. Frąckowiak:** Investigation, Data curation, Visualization. **M. Koterlyn:** Conceptualization, Resources. **J. Sebesta:** Methodology, Software, Investigation, Data curation, Writing – review & editing, Visualization. **D. Legut:** Methodology, Software, Investigation, Data curation, Writing – review & editing, Visualization. **T. Toliński:** Conceptualization, Resources, Writing – original draft, Supervision, Project administration, Funding acquisition.

Declaration of Competing Interest

The authors declare that they have no known competing financial interests or personal relationships that could have appeared to influence the work reported in this paper.

Acknowledgements

DL and JS acknowledge support by the ERDF in the IT4Innovations national supercomputing center – path to exascale project (CZ.02.1.01/0.0/0.0/16_013/0001791) within the OPRDE and the e-INFRA CZ project (ID:90140) by the Ministry of Education, Youth and Sports of the Czech Republic.

References:

[1] C. Grazioli, Z. Hu, M. Knupfer, G. Graw, G. Behr, M.S. Golden, J. Fink, H. Giefers, G. Wortmann, K. Attenkofer, Characteristic temperature dependence of the 4f occupancy in the Kondo system $CeSi_2$, Phys. Rev. B 63 (2001), 115107, https://doi.org/10.1103/PhysRevB.63.115107.

[2] J.M. Lawrence, J.W. Allen, S.-J. Oh, I. Lindau, Resonant photoemission in CeAl, $CeSi_2$, and $LaSi_2$, Phys. Rev. B 26 (1982) 2362–2370, https://doi.org/10.1103/PhysRevB.26.2362.

[3] M.M. Sánchez-López, J. Costa-Quintana, E. González-León, F. López-Aguilar, L. Puig-Puig, Electronic structure of $CeSi_2$, Physica B 199–200 (1994) 202–203, https://doi.org/10.1016/0921-4526(94)91782-5.

[4] A.V. Morozkin, V.A. Stupnikov, V.N. Nikiforov, N. Imaoka, I. Morimoto, Thermoelectric properties of the solid solutions based on $ThSi_2$-type $CeSi_2$ compound, J. Alloy. Compd. 415 (1-2) (2006) 12–15, https://doi.org/10.1016/j.jallcom.2005.07.053.

[5] S.K. Dhar, S.M. Pattalwar, R. Vijayaraghavan, Structural and magnetic properties of $CeSi_{2-x}Ga_x$ alloys (x=1.5, 1.75 and 2.0), Solid State Commun. 87 (5) (1993) 409–411, https://doi.org/10.1016/0038-1098(93)90787-N.

[6] S.K. Dhar, Magnetic studies of $Ce_{1-x}Ga_{2(1+x)}$ (x = 0, 0.2 and 0.3) alloys, J. Magn. Magn. Mater. 129 (2-3) (1994) 259–262, https://doi.org/10.1016/0304-8853(94)90118-X.

[7] M. Takahashi, H. Tanaka, T. Satoh, M. Kohgi, Y. Ishikawa, T. Miura, H. Takei, Multiple phase transitions of single crystalline $CeGa_2$, J. Phys. Soc. Jpn. 57 (4) (1988) 1377–1383, https://doi.org/10.1143/JPSJ.57.1377.

[8] P. Burlet, M.A. Frémy, D. Gignoux, G. Lapertot, S. Quezel, L.P. Regnault, J. Rossat-Mignod, E. Roudaut, Magnetic properties of the Kondo lattice $CeGa_2$, J. Magn. Magn. Mater. 63–64 (1987) 34–36, https://doi.org/10.1016/0304-8853(87)90513-0.

[9] K. Shashikala, A. Sathyamoorthy, P. Raj, S.K. Dhar, S.K. Malik, Structure and magnetic properties of $CeGa_2D_{0.6}$ system, J. Alloy. Compd. 436 (1-2) (2007) 19–22, https://doi.org/10.1016/j.jallcom.2006.07.047.

[10] Y. Çiftci, K. Çolakoğlu, C. Çoban, E. Deligöz, The structural, elastic and thermodynamic properties of intermetallic compound $CeGa_2$, Open, Physics. 10 (2012) 197–205, https://doi.org/10.2478/s11534-011-0012-9.

[11] H. Mori, N. Sato, T. Sato, An electronically-driven volume transition in $CeSi_{2-x}Ga_x$, Solid State Commun. 49 (1984) 955–958, https://doi.org/10.1016/0038-1098(84)90301-6.

[12] V.V. Moshchalkov, O.V. Petrenko, M.K. Zalyalyutdinov, The new Kondo lattice compounds: $CeSi_{2-x}Ga_x$, Physica B 163 (1-3) (1990) 395–397, https://doi.org/10.1016/0921-4526(90)90222-G.

[13] K.R. Priolkar, S.M. Pattalwar, P.K. Mishra, P. Raj, A. Sathyamoorthy, S.K. Dhar, V. C. Sahni, P.R. Sarode, R.B. Prabhu, Structural and magnetic behaviour of $CeSi_{0.6}Ga_{1.4}$, Solid State Commun. 104 (2) (1997) 71–73, https://doi.org/10.1016/S0038-1098(97)00307-4.

[14] K.R. Priolkar, M.N. Rao, R.B. Prabhu, P.R. Sarode, S.K. Paranjpe, P. Raj, A. Sathyamoorthy, Spin dynamics of $CeSi_{2-x}Ga_x$, $0.7 \leqslant x \leqslant 1.3$, J. Magn. Magn. Mater. 185 (3) (1998) 375–378, https://doi.org/10.1016/S0304-8853(98)00039-0.

[15] K.R. Priolkar, R.B. Prabhu, P.R. Sarode, V. Ganesan, P. Raj, A. Sathyamoorthy, Competition between RKKY and Kondo interactions in $CeSi_{2-x}Ga_x$, J. Phys.: Condens. Matter 10 (20) (1998) 4413–4422, https://doi.org/10.1088/0953-8984/10/20/009.

[16] G.M. Darone, B. Hmiel, J. Zhang, S. Saha, K. Kirshenbaum, R. Greene, J. Paglione, S. Bobev, Rare-earth metal gallium silicides via the gallium self-flux method. Synthesis, crystal structures, and magnetic properties of $RE(Ga_{1-x}Si_x)_2$ (RE=Y, La–Nd, Sm, Gd–Yb, Lu), J. Solid State Chem., 201 (2013) 191–203. doi: 10.1016/j.jssc.2013.02.029.

[17] R. Pöttgen, B. Chevalier, Equiatomic cerium intermetallics CeXX′ with two p elements, Zeitschrift Für Naturforschung B 70 (2015) 695–704, https://doi.org/10.1515/znb-2015-0109.

[18] K.R. Priolkar, M.N. Rao, R.B. Prabhu, P.R. Sarode, S.K. Paranjpe, P. Raj, A. Sathyamoorthy, Inelastic neutron scattering in $CeSi_{2-x}Ga_x$ ferromagnetic Kondo lattice compounds, J. Phys.: Condens. Matter 10 (1998) 10557–10564, https://doi.org/10.1088/0953-8984/10/47/007.

[19] A. Kitanovski, Energy applications of magnetocaloric materials, Adv. Energy Mater. 10 (10) (2020) 1903741, https://doi.org/10.1002/aenm.v10.1010.1002/aenm.201903741.

[20] J. Mao, G. Chen, Z. Ren, Thermoelectric cooling materials, Nat. Mater. 20 (4) (2021) 454–461, https://doi.org/10.1038/s41563-020-00852-w.

[21] A.S. Erchidi Elyacoubi, R. Masrour, A. Jabar, Magnetocaloric effect and magnetic properties in $SmFe_{1-x}Mn_xO_3$ perovskite: Monte Carlo simulations, Solid State Commun. 271 (2018) 39–43, https://doi.org/10.1016/j.ssc.2017.12.015.

[22] G. Kadim, R. Masrour, A. Jabar, E.K. Hlil, Room-temperature large magnetocaloric, electronic and magnetic properties in $La_{0.75}Sr_{0.25}MnO_3$ manganite: ab initio calculations and Monte Carlo simulations, Physica A 573 (2021) 125936, https://doi.org/10.1016/j.physa:2021.125936.

[23] L.M. Moreno-Ramírez, V. Franco, Setting the basis for the interpretation of temperature first order reversal curve (TFORC) distributions of magnetocaloric materials, Metals 10 (2020) 1039, https://doi.org/10.3390/met10081039.

[24] J. Rodríguez-Carvajal, Recent advances in magnetic structure determination by neutron powder diffraction, Physica B 192 (1-2) (1993) 55–69, https://doi.org/10.1016/0921-4526(93)90108-I.
[25] W. Kohn, N. Rostoker, Solution of the Schrödinger equation in periodic lattices with an application to metallic lithium, Phys. Rev. 94 (5) (1954) 1111–1120, https://doi.org/10.1103/PhysRev.94.1111.
[26] H. Ebert, D. Ködderitzsch, J. Minár, Calculating condensed matter properties using the KKR-Green's function method—recent developments and applications, Rep. Prog. Phys. 74 (9) (2011) 096501, https://doi.org/10.1088/0034-4885/74/9/096501.
[27] S.H. Vosko, L. Wilk, M. Nusair, Accurate spin-dependent electron liquid correlation energies for local spin density calculations: a critical analysis, Can. J. Phys. 58 (8) (1980) 1200–1211, https://doi.org/10.1139/p80-159.
[28] H. Ebert, A. Perlov, S. Mankovsky, Incorporation of the rotationally invariant LDA +U scheme into the SPR-KKR formalism: application to disordered alloys, Solid State Commun. 127 (6) (2003) 443–446, https://doi.org/10.1016/S0038-1098(03)00455-1.
[29] J. Åhman, G. Svensson, J. Albertsson, A reinvestigation of β-gallium oxide, Acta Crystallogr. C Cryst. Struct. Commun. 52 (1996) 1336–1338, https://doi.org/10.1107/S0108270195016404.
[30] D. Louër, Advances in powder diffraction analysis, Acta Crystallogr. A Found. Crystallogr. 54 (1998) 922–933, https://doi.org/10.1107/S0108767398007363.
[31] M. Bałanda, AC susceptibility studies of phase transitions and magnetic relaxation: conventional, molecular and low-dimensional magnets, Acta Phys. Pol. A 124 (2013) 964–976, https://doi.org/10.12693/APhysPolA.124.964.
[32] P. Skokowski, K. Synoradzki, M. Werwiński, T. Toliński, A. Bajorek, G. Chełkowska, Influence of Pr substitution on the physical properties of the $Ce_{1-x}Pr_xCoGe_3$ system: Combined experimental and first-principles study, Phys. Rev. B 102 (2020), 245127, https://doi.org/10.1103/PhysRevB.102.245127.
[33] J.M.D. Coey, Magnetism and Magnetic Materials, Cambridge University Press, Cambridge, 2010.
[34] E. Bauer, M. Rotter, Magnetism of complex metallic alloys: crystalline electric field effects, in: Book Series on Complex Metallic Alloys, World Scientific, 2009: pp. 183–248. doi: 10.1142/9789814261647_0005.
[35] A. Arrott, Criterion for ferromagnetism from observations of magnetic isotherms, Phys. Rev. 108 (6) (1957) 1394–1396, https://doi.org/10.1103/PhysRev.108.1394.
[36] V. Franco, J.S. Blázquez, J.J. Ipus, J.Y. Law, L.M. Moreno-Ramírez, A. Conde, Magnetocaloric effect: from materials research to refrigeration devices, Prog. Mater Sci. 93 (2018) 112–232, https://doi.org/10.1016/j.pmatsci.2017.10.005.
[37] L.C. Wang, Q.Y. Dong, J. Lu, X.P. Shao, Z.J. Mo, Z.Y. Xu, J.R. Sun, F.X. Hu, B. G. Shen, Low-temperature large magnetocaloric effect in the antiferromagnetic CeSi compound, J. Alloy. Compd. 587 (2014) 10–13, https://doi.org/10.1016/j.jallcom.2013.10.183.
[38] R.D. dos Reis, L.M. da Silva, A.O. dos Santos, A.M.N. Medina, L.P. Cardoso, F. G. Gandra, Study of the magnetocaloric properties of the antiferromagnetic compounds RGa_2 (R = Ce, Pr, Nd, Dy, Ho and Er), J. Phys.: Condens. Matter 22 (48) (2010) 486002, https://doi.org/10.1088/0953-8984/22/48/486002.
[39] V. Franco, J.S. Blázquez, A. Conde, Field dependence of the magnetocaloric effect in materials with a second order phase transition: a master curve for the magnetic entropy change, Appl. Phys. Lett. 89 (22) (2006) 222512, https://doi.org/10.1063/1.2399361.
[40] A. Tari, The specific heat of matter at low temperatures, Imperial College Press ; Distributed by World Scientific Pub. Co, London : River Edge, NJ, 2003.
[41] M.B. Fontes, J.C. Trochez, B. Giordanengo, S.L. Bud'ko, D.R. Sanchez, E.M. Baggio-Saitovitch, M.A. Continentino, Electron-magnon interaction in RNiBC (R = Er, Ho, Dy, Tb, and Gd) series of compounds based on magnetoresistance measurements, Phys. Rev. B 60 (1999) 6781–6789, https://doi.org/10.1103/PhysRevB.60.6781.
[42] M.B. Tchoula Tchokonté, J.J. Mboukam, A.K.H. Bashir, B.M. Sondezi, K.R. Kumar, A.M. Strydom, D. Kaczorowski, Electrical resistivity and thermodynamic properties of the ferromagnet Nd_2Pt_2In, J. Alloy. Compd. 753 (2018) 41–45, https://doi.org/10.1016/j.jallcom.2018.04.193.
[43] J.J. Mboukam, B.M. Sondezi, M.B.T. Tchokonté, A.K.H. Bashir, A.M. Strydom, D. Britz, D. Kaczorowski, Magnetocaloric effect and other low-temperature properties of Pr_2Pt_2In, Physica B 536 (2018) 505–509, https://doi.org/10.1016/j.physb.2017.07.069.
[44] D. Das, D. Gnida, Ł. Bochenek, A. Rudenko, M. Daszkiewicz, D. Kaczorowski, Magnetic field driven complex phase diagram of antiferromagnetic heavy-fermion superconductor Ce_3PtIn_{11}, Sci. Rep. 8 (2018) 16703, https://doi.org/10.1038/s41598-018-34991-7.
[45] K. Synoradzki, D. Das, A. Frąckowiak, D. Szymański, P. Skokowski, D. Kaczorowski, Study on magnetocaloric and thermoelectric application potential of ferromagnetic compound $CeCrGe_3$, J. Appl. Phys. 126 (7) (2019) 075114, https://doi.org/10.1063/1.5107450.
[46] V. Nikiforov, V. Irkhin, A. Morozkin, Thermoelectricity in Ternary Rare-Earth Systems, in: R. Egger, D. Matrasulov, K. Rakhimov (Eds.), Low-Dimensional Functional Materials, Springer Netherlands, Dordrecht, 2013: pp. 235–242. doi: 10.1007/978-94-007-6618-1_19.